Colloid Polym Sci (2006) 285: 19–25
DOI 10.1007/s00396-006-1525-4

ORIGINAL CONTRIBUTION

Francesca Bellezza
Antonio Cipiciani
Umberto Costantino
Fabio Marmottini
Maria Anna Quotadamo

Zirconium phosphate nanoparticles from water-in-oil microemulsions

Received: 27 March 2006
Accepted: 24 May 2006
Published online: 3 August 2006

F. Bellezza · A. Cipiciani (✉) ·
U. Costantino · F. Marmottini ·
M. A. Quotadamo
Centro di Eccellenza Materiali
Innovativi Nanostrutturati (CEMIN),
Dipartimento di Chimica,
Università di Perugia,
Via Elce di Sotto,
06123 Perugia, Italy
e-mail: cipan@unipg.it
Tel.: +39-75-5855540
Fax: +39-75-5855560

Abstract Non-ionic water-in-oil (w/o) microemulsions of pentaoxyethyl-enenonylphenyl ether (Igepal-CO520)/cyclohexane/water at 25 °C have been used as reaction vessels to obtain zirconium hydrogen phosphate nanoparticles.

Keywords Zirconium phosphate · Nanoparticles · Microemulsions

Introduction

The development of nanotechnologies requires the use of materials at nanometric scale and several synthetic routes (vapor-phase synthesis [1], coprecipitation [2], sol–gel and hydrothermal methods [3, 4]) have been proposed for the preparation of nanoparticles of different materials of interest in technological applications.

Among the many synthetic routes, the one based in water-in-oil (w/o) microemulsions has been widely used in the preparation of colloidal inorganic nanocrystals as microemulsions can be considered nanosized reaction chambers that are especially suited for the controlled nucleation and growth of inorganic precipitates [5]. Water-in-oil microemulsions are transparent, isotropic liquid media with very small water droplets dispersed in a continuous oil phase and stabilized by surfactant molecules at the water/oil interface. The water droplets, enveloped by surfactant molecules, offer a unique microenvironment for the formation of nanoparticles. They not only act as microreactors for processing reactions but also control the aggregation of particles because the surfactant molecules could be adsorbed onto the particle surface when the particle size approaches that of water-pool. In this way, the resultant coated particles are generally very fine and monodispersed [6].

The synthesis of colloidal nanoparticles using w/o microemulsions has been reported for many inorganic materials, including metals [7], metal sulfides [8], carbonates [9], halides [10], oxides [11], and hydroxides [12]. Recently, studies have been reported on the synthesis of zirconia [13] and sulphated-zirconia [14] nanoparticles in reverse microemulsions, but there are no reports of the preparation of zirconium phosphate nanoparticles, notwithstanding the large interest in zirconium phosphates and phosphonates chemistry.

Amorphous and crystalline zirconium phosphates, hereafter indicated as ZrP, have been found to possess a high cation exchange capacity and good stability to acid and oxidizing solutions, to relatively high temperatures and to ionizing radiations [15]. Zirconium phosphates behave as pure solid-state proton conductors, intercalating agents of protophilic species, fillers of polymeric nanocomposites and supports to bind enzyme and proteins

[16–18]. A very attractive aspect of zirconium phosphate chemistry is related to the possibility of replacing the P-OH groups anchored to the layer surface of crystalline α-$Zr(HPO_4)_2{\cdot}H_2O$ with P-OR or P-R groups without altering the inorganic texture of the layer (R is an organic group) [19]. The layered compounds so obtained are considered organic derivatives of the parent $Zr(HPO_4)_2{\cdot}H_2O$ with the layers being functionalized with a large variety of organic groups (alkyl, aryl, carboxylic, aminoacidic, sulfophenyl).

This paper is concerned with the preparation of zirconium phosphate (ZrP) nanoparticles with the double-microemulsion technique and with the characterization of the obtained material.

This technique consists of mixing two microemulsions, each containing one of the ions forming the precipitate [20]; the intermicellar exchange of solutes is essential for product formation. The droplets are indeed subject to Brownian motion and collide continuously, leading to the formation of short-lived dimers and the exchange of the aqueous contents of the reverse micelles. This dynamic process ensures a homogeneous repartitioning of the reactants among the water pools of the droplets, and thus the formation of mono-dispersed particles [20].

A typical w/o microemulsion of non-ionic surfactant (Igepal-CO520)/cyclohexane/water was used in the present work The microemulsions were studied by dynamic light scattering before and after the mixing of the reactant species present in the water pools. The particle sizes of the obtained nanoparticles were investigated by transmission electron microscopy (TEM). The obtained powder products were studied by chemical and thermogravimetric analyses, by scanning electron microscopy (SEM), and by X-ray diffraction experiments.

Experimental

Materials

$ZrOCl_2{\cdot}8H_2O$ was a Merck “pro analysi” product and H_3PO_4 (85%) a Carlo Erba RP-ACS reagent. Igepal-CO520 (pentaoxyethylene nonyl phenyl ether) and cyclohexane were Sigma-Aldrich products.

Synthesis of ZrP nanoparticles in microemulsion

Solutions of Igepal in cyclohexane (0.15 M) were first prepared, then the two microemulsions, designated μA and μB, were obtained by adding a 0.15-M $ZrOCl_2$ aqueous solution (μA) or a 1.2-M H_3PO_4 acqueous solution (μB), respectively. The volumes of aqueous solutions were selected to have the desired water-to-surfactant molar ratio R_W and oil-to-water molar ratio R_O.

The double-microemulsion processing route was then carried out by mixing equal volumes of μA and μB to obtain the precipitation of ZrP particles, in large excess of phosphoric acid, in the reverse micelles. The resulting system, called μAB, was aged at room temperature. After aging, the particles were recovered by centrifuging and a semi-transparent gel was obtained. The gel, about 1 g, was washed with cyclohexane (3×50 ml), with ethanol (3×50 ml) and then was dried at 80 °C under oil pump vacuum to give a white powder.

Characterization of microemulsions

Dynamic light-scattering experiments were carried out to estimate the micellar size of the reverse microemulsions, before and after the mixing of the reactants.

The measurements were made by using approximately 1 ml of sample in 6-mm diameter Pyrex glass culture tubes, protected from dust by parafilm caps. The cylindrical glass sample tube was fixed at the center of a toluene-filled fluorimeter cuvette to provide refractive index matching against stray light reflections. The cuvette was housed in a black-anodized aluminum cell block, whose temperature was regulated by a Peltier thermoelectric element. The light source was a Coherent Innova 70-3 Argon-ion laser, operating at 4,880Å. Light scattered at 90° was collected from approximately one coherence area and projected onto the slit of a photomultiplier tube (Products for Research). A 64-channel Nicomp Model 370 computing autocorrelator was used to calculate and display the diffusion coefficient, D, and to associate the derived parameters from the cumulants analysis [21] to the intensity autocorrelation function. All measurements showed reasonable goodness-of-fit values. The hydrodynamic radii, R_h, were estimated by applying the Stokes–Einstein relation (for stick-boundary conditions) [22]:

$$D = kT/6\pi\eta R_h$$

where η is the viscosity of the solution (often approximated to that of pure water) and k the Boltzmann constant.

Characterization of nanoparticles

The morphology of the ZrP particles dispersed in the microemulsion was studied using a Philips 208 Transmission Electron Microscope (TEM). A small drop of microemulsion was deposited on a copper grid pre-coated with a Formvar film and then evaporated in air at room temperature. Dried powders were studied with chemical analysis, X-ray powder diffraction, thermal analysis, specific surface area, and particle size and shape.

Phosphate analysis was performed by Ion Chromatography using a Dionex 500 instrument with a Dionex AS4A column. The same instrument, with a Dionex 201 TP column, was used for the determination of zirconium following the procedure described in reference [23] (Eluent: acetonitrile/water 55/45 V/V with acetic acid/ sodium acetate at pH 4, flux: 1.0 ml/min, detection: spectrophotometric at 585 nm).

The X-ray powder diffraction (XRPD) patterns were taken with a computerized Philips PW1710 diffractometer using the CuKα radiation, operating at 40 kV and 20 mA, step scan 1° min^{-1}. The specific surface areas were calculated according to the B.E.T. method from N_2 adsorption isotherms taken at 77 K with a computer-controlled Micromeritics ASAP2010 instrument.

Coupled thermogravimetric (TGA) and differential thermal (DTA) analyses were performed with a Netzsch STA 449C thermobalance, in air flow and heating rate of 10 °C/min. Particle shape and size were obtained with a Philips XL30 Scanning Electron Microscope (SEM).

Results and discussion

Synthesis of ZrP nanoparticles with the two-microemulsions technique

Much of the work involving microemulsion-based synthesis of nanoparticles has been done with the anionic amphiphilic surfactant AOT [sodium bis(2-ethylhexyl) sulfosuccinate], as it is very efficient in solubilizing water into surfactant–hydrocarbon mixtures [24]. However, the solubilizing capacity of AOT is severely reduced when the aqueous phase is a solution with a high concentration of cations or protons.

Non-ionic surfactants, like ethoxylates alcohols, are much less sensitive to the presence of cations and their water-solubilization capacity is almost the same in the absence or presence of electrolyte solutes [25]. Taking into account the nature of the reactants ($ZrOCl_2$ and H_3PO_4), it was decided to use a non-ionic surfactant, and in particular, Igepal CO-520 (polyoxyethylene moiety with a terminal hydroxyl group as a polar part and a long hydrocarbon chain as a tail part) and the two-emulsion technique was employed to obtain the precipitation of zirconium phosphate nanoparticles. The precipitation reaction takes place in the core of the reverse micelles and when the size of the precipitate approaches that of water-pool the physical interactions between the particles surface and the hydrophilic head groups of the surfactant molecules can stop the growth of the nanoparticles.

The microemulsion composition can be varied to tailor the properties of the derived nanoparticles. In a first approximation, the amount of water influences the primary particle sizes as the inverse micelle sizes depend on the water-to-surfactant molar ratio, R_w.

$$R_w = n(H_2O)/n(\text{Surfactant})$$

The ability of the surfactant–alkane mixtures to solubilize water is limited and varies with the structure of the surfactant, the oil phase and the temperature. Therefore, R_w values are not sufficient to characterize the microemulsion system. Another important parameter that affects the separation of micelles is the oil-to-water molar ratio, R_O.

$$R_O = n(\text{Oil})/n(H_2O)$$

Several experiments were carried out by changing the relative amount of oil, water, surfactant and reactants to have clear and stable microemulsions. The composition of microemulsions (those containing $ZrOCl_2$ and those

Table 1 Composition of the microemulsions used for the synthesis of zirconium phosphate nanoparticles at room temperature

Entry	Sample	[S][a] (wt%)	[O][a] (wt%)	[W][a] (wt%)	$ZrOCl_2$ (M)[b]	H_3PO_4 (M)[b]	R_W	R_O
1	A	6	92	2	0.15	–	6	10
	B	6	92	2	–	1.2	6	10
2	A	6	90	4	0.15	–	14	4
	B	6	90	4	–	1.2	14	4
3	A	11	86	3	0.3	–	5	6
	B	11	86	3	–	2.4	5	6
4	A	11	83	6	0.3	–	9	3
	B	11	83	6	–	2.4	9	3
5	A	15	83	2	0.6	–	2	12
	B	15	83	2	–	4.8	2	12
6	A	15	80	5	0.6	–	5	4
	B	15	80	5	–	4.8	5	4

[a] *S* Surfactant, *O* oil, *W* water
[b] Concentrations were in reference to the total volume of the aqueous phase

containing H_3PO_4 designated A and B, respectively) are listed in Table 1. In all the experiments, the resulting mixtures obtained by mixing the microemulsions (A and B) were transparent. Therefore, the precipitation of ZrP particles was expected to take place in the nanosized aqueous domains. The reverse microemulsions remained transparent even after 16 h of aging although the formation of colloidal particles of zirconium phosphate very likely occurs soon after the mixing of the two microemulsions. These experiments showed that it is possible to obtain ZrP particles in a large interval of R_O and R_W values and that it is possible to collect them by centrifugation (see later). The study of the effect of the parameters that control the microemulsions on the formation of the colloidal particles was out of the aim of the present work and it was decided to study and characterize only the colloidal particles obtained with the experiment of entry 1 of Table 1.

Figure 1 shows the TEM image of particles obtained after 1 h of aging (experiment: entry 1 of Table 1). The particles have the shape of nanospheres and their sizes vary from 10 to 100 nm.

Dynamic light-scattering experiments were performed for Igepal-based microemulsions containing $ZrOCl_2$ and H_3PO_4 aqueous solutions obtained according the experiment described in Table 1, entry 1. The results provided radii of 17.8±3.6 and 27.9±5.6 nm, respectively.

The droplet hydrodynamic radii of the microemulsions obtained immediately after mixing of the two reactants and after 1 h of aging were similar (25.3±5.2 nm). Therefore, there was no increase nor decrease in the water-pool size after ZrP particles precipitation.

After 16 h of aging, the microemulsions were still transparent, but TEM analysis revealed that the particle size had increased slightly with some particle aggregation appearing (Fig. 2). Note that the dimensions of the microemulsion-based nanoparticles obtained with light-scattering experiments agree well with those obtained by TEM analysis.

It was of interest to evaluate the order of magnitude of the specific surface area, which can be expected for the nanoparticles obtained immediately after mixing solutions A and B. Such an estimate can be based on the following stoichiometric considerations.

1) The spherical particles of A and B microemulsions have a volume (V), calculated from the results of the light-scattering experiments, equal to $4/3\pi(17.8)^3=2.36\ 10^4$ nm^3 and $4/3\pi(27.9)^3=9.09\ 10^4$ nm^3, respectively. These volumes refer to the surfactant Stern layer and to the aqueous solutions of $ZrOCl_2$ 0.15 M and H_3PO_4 1.2 M, respectively. If the thickness of the Stern layer is not considered, each reactant droplet contains $3.54\ 10^{-21}$ mol of $ZrOCl_2$ and $1.09\ 10^{-19}$ mol of H_3PO_4, respectively.
2) After mixing the two microemulsions, it is assumed that all the zirconium is precipitated as zirconium phosphate. Therefore, each new droplet should contain $3.54\ 10^{-21}$ mol of zirconium phosphate. By assuming that the precipitate has the formula $Zr(HPO_4)_2$ and a density of 2.72 g/cm^3 (density of the zirconium bis (monohydrogenphosphate) with α-layered structure [26]), each ZrP nanoparticle should have a mass of $9.9\ 10^{-19}$ g and a volume of $3.64\ 10^{-19}$ cm^3. Therefore, assuming a spherical-shaped precipitate, a surface area of $2.5\ 10^{-12}$ cm^2 may be evaluated for each nanoparticle by means of the formula $S=4\pi(3V/4\pi)^{2/3}$. In conclusion, a surface area of 252 m^2/g can be obtained for the ZrP dispersion in microemulsion.

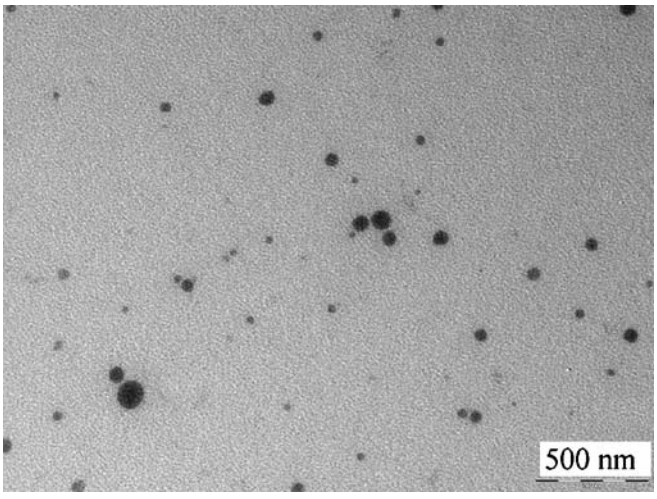

Fig. 1 TEM micrograph of zirconium phosphate nanoparticles, obtained from the experiment described in entry 1 of Table 1, after 1 h of aging

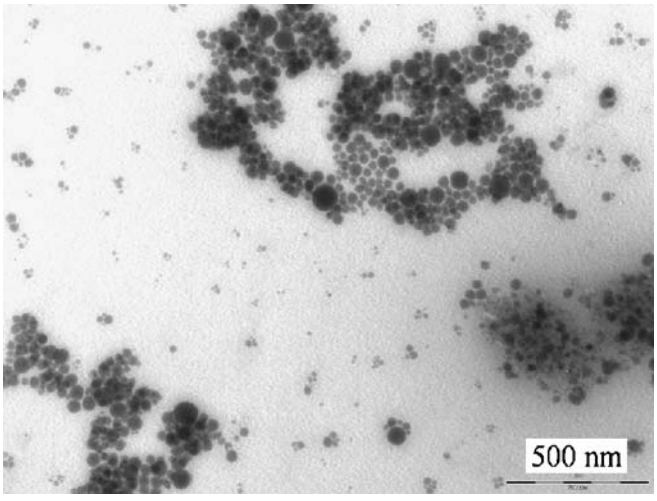

Fig. 2 TEM micrograph of zirconium phosphate nanoparticles, obtained from the experiment described in entry 1 of Table 1, after 16 h of aging

On the basis of these considerations, it was decided to recover the nanoparticles from the reverse micelles to carry out their physical–chemical characterization.

Physical–chemical characterization of the recovered and dried nanoparticles

The particles obtained from the experiment described in entry 1, Table 1 were recovered by centrifugation after 16 h of aging. The semi-transparent gel obtained was washed with cyclohexane and ethanol to remove the excess surfactant and then dried.

Figure 3 shows the XRD patterns of the obtained dried gel. The broad diffraction maxima of low intensity present on the pattern can be related to the reflection broadening by the extremely small particles sizes and probably also by considerable structural disorder [27].

The nanoparticles have a P/Zr molar ratio of 2.1 (determined as described in the experimental). This value is a little higher than that derived from the stoichiometric formula. This value indicates the presence of strongly absorbed phosphoric acid or the presence of some dihydrogen phosphate groups together with the monohydrogen phosphate groups.

Figure 4 shows the TGA and DTA analyses of the recovered nanoparticles. The TGA curve indicates three steps of weight loss: the first one appears at about 150 °C and corresponds to the elimination of adsorbed water and solvent; the second one, corresponding to the surfactant degradation, occurs at temperatures around 300 °C; and the third step occurs at temperatures higher than 500 °C and corresponds to water loss due to the condensation of the hydrogen-phosphates groups and to the oxidation of carbonaceous deposits. If we consider that the residual in the thermogrammetric curve at 1,000 °C is cubic zirconium pyrophosphate, the surfactant content in the initial solid can be estimated to be about 50% w/w, corresponding to about 1.4 mol of Igepal CO520 per mol of zirconium.

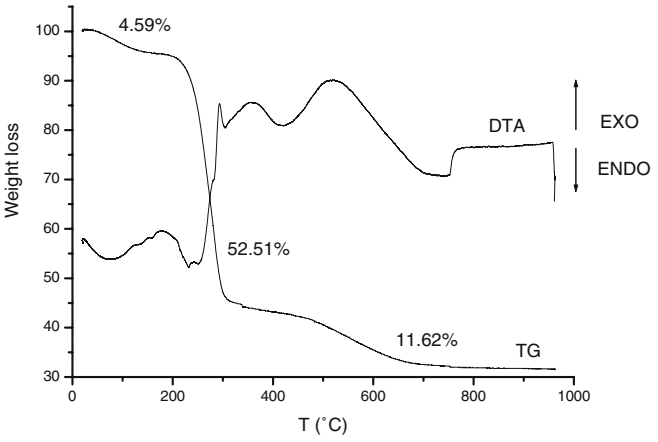

Fig. 4 Thermogravimetric analysis (TGA) and differential thermal analysis (DTA) of zirconium phosphate particles (air flow and heating rate of 10 °C/min)

SEM micrographs of recovered solid are shown in Fig. 5. The particle size of a few micrometers indicates that the nanoparticles present in the microemulsion tend to aggregate. Hence, the recovered particles are covered by a film of surfactant molecules that could also have been intercalated.

The elimination of the organic residues in the solid should leave the inorganic zirconium phosphate. With this aim, we decided to investigate the following two procedures for removing the adsorbed molecules of surfactant:

a) calcination at different temperatures
b) washing with KOH 0.01 M.

When the surfactant was removed by calcination, at 400 and 600 °C, different results were obtained. At 400 °C, the

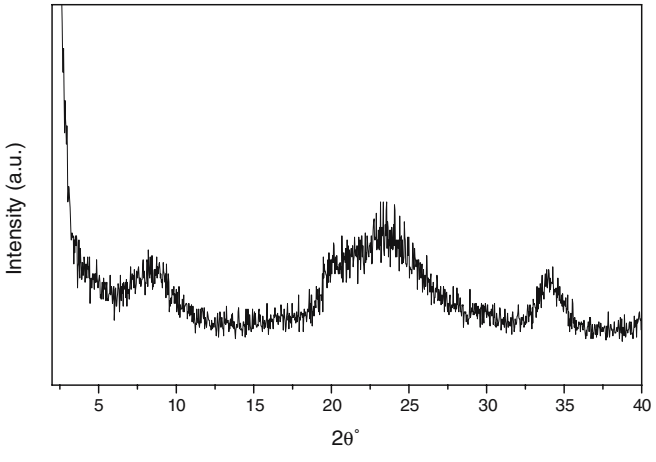

Fig. 3 XRD patterns of zirconium phosphate particles recovered from reverse microemulsions

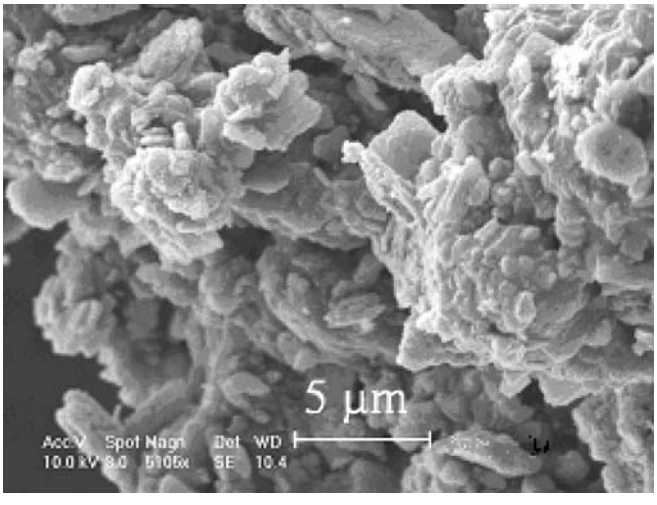

Fig. 5 SEM micrograph of zirconium phosphate particles

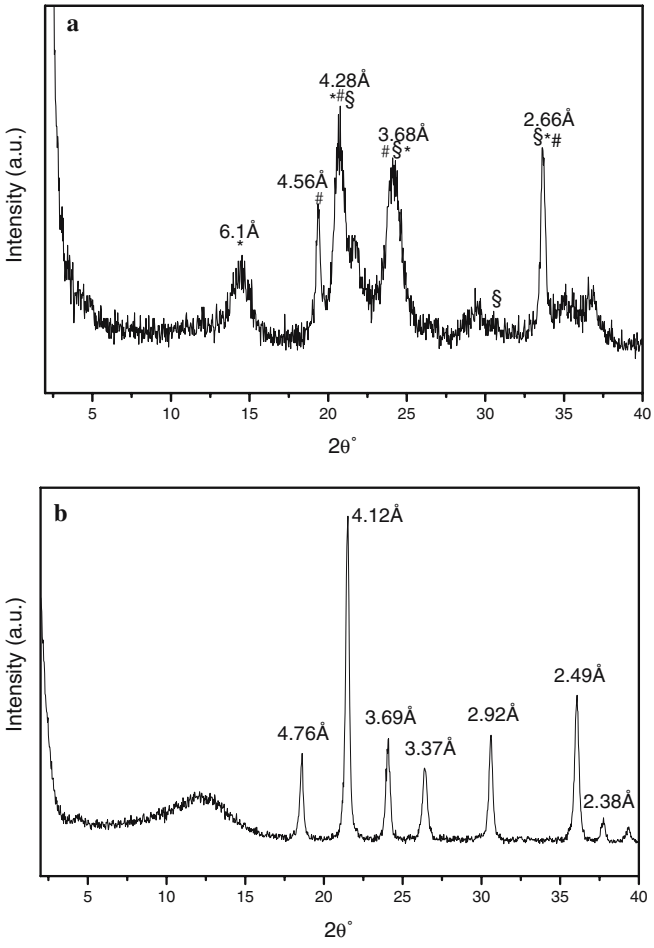

Fig. 6 XRD patterns of zirconium phosphate particles after calcinations at **a** 400 °C and **b** 600 °C. In figures the following symbols indicate X-ray reflections attributable to: *asterisk* layered zirconium pyrophosphate [28]; *§* cubic zirconium phosphate; # anhydrous zirconium hydrogen phosphate

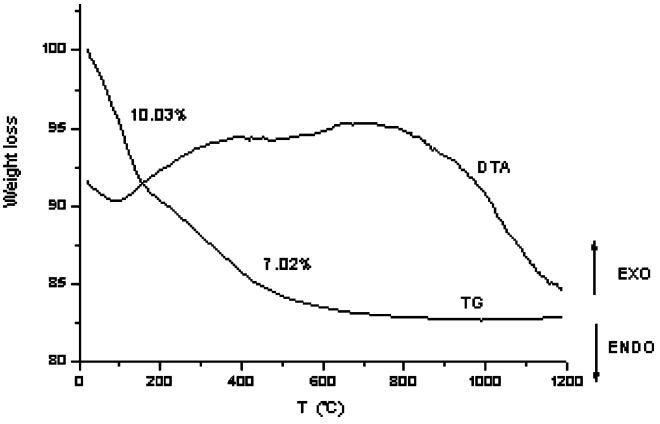

Fig. 7 Thermogravimetric analysis (*TGA*), differential thermal analysis (*DTA*), and differential thermogravimetric (*DTG*) curve of zirconium phosphate obtained after washing the recovered particles with KOH solution

organic residue was degraded and partially converted into carbonaceous species. B.E.T. analysis indicated the presence of a microporous material with a surface area of 224 m^2/g, which was probably affected by the presence of coke.

After calcination at 600 °C, the coke was almost completely removed from the surface of the particles and the measured B.E.T. surface area decreased to 47 m^2/g.

The XRD patterns of the samples heated at 400 and 600 °C are shown in Fig. 6a and b, respectively.

The comparison between these patterns with that of the pristine material (see Fig. 3) indicates that the heating induces the crystallization of the particles, associated to the loss of condensation water of hydrogen phosphate to pyrophosphate groups. In fact, the pattern shown in Fig. 6b is typical of cubic zirconium pyrophosphate [28], while the pattern of Fig. 6a contains some broad and weak together with sharper reflections attributable to layered zirconium pyrophosphate [28], cubic zirconium pyrophosphate, and very likely to semi-crystalline anhydrous zirconium hydrogen phosphate (see symbols in Fig. 6). Hence, the sample heated at 400 °C, not yet well crystallized, is polyphasic and may be considered an intermediate product between the colloidal nanoparticles and the crystalline ZrP_2O_7.

We also tried to remove the adsorbed molecules of the non-ionic surfactant Igepal CO-520 from the hydrophilic surface of ZrP by washing the precipitate gel with a solution of KOH 0.01 M for 3 h. The solid was recovered by centrifugation and dried.

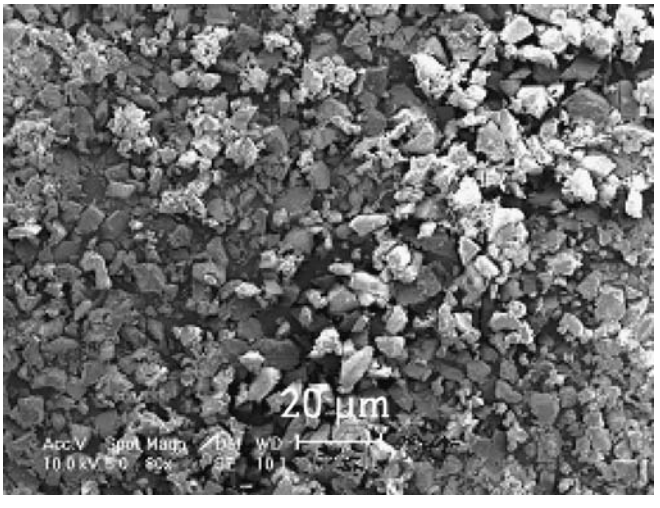

Fig. 8 SEM micrograph of zirconium phosphate obtained after washing the recovered particles with KOH solution

Thermal analysis (Fig. 7) revealed the presence of a very small amount of surfactant molecules in the sample. The alkaline washing seemed to be an efficient way to remove the surfactant from the surface of the particles, favoring their aggregation. In this context, it is noteworthy to observe that the B.E.T. surface analysis of the particles after alkaline washing and drying (51 m^2/g) was similar to that of the particles calcinated at 600 °C (47 m^2/g). Furthermore, the aggregation leads to the formation of particles of about 1 micron that are well visible in the SEM micrograph of the powder shown in Fig. 8.

Conclusions

Nanosized ZrP particles can be prepared in reverse microemulsion system using $ZrOCl_2$ and H_3PO_4 as reagents. The nanoparticles are rapidly formed and are stable over time. The size of the colloidal particles can be controlled by the size of the core of the reverse micelles. In contrast, the separation of the nanoparticles from the reaction medium produces a gel made up of particles coated with surfactant molecules. The gel-like aggregation of the small particles with an estimated specific surface area of 252 m^2/g reduces considerably the specific area of the dried gel. Attempts to remove the surfactant by calcination or by washing with alkaline solution provided particles that were essentially without organic surfactant but at the same time induced reaggregation phenomena with an increase in size and a further decrease in surface area. However, the two microemulsions method could give rise to the suspension of nanoparticles in different media and could be extended to the preparation of zirconium phosphonates with different functional groups on the surface.

Acknowledgements The authors express their gratitude to Dott. P. Di Profio for providing light-scattering measurements. Two of the authors (U.C., F.M.) thank MUIR (PRIN 2004) for financial support.

References

1. Swihart MT (2003) Curr Opin Colloid Interface Sci 8:127
2. Tang ZX, Sorensen CM, Klabunde KJ, Hadjipanays GC (1991) J Colloid Interface Sci 146:38
3. Yang X, He Q, He X, Huang L (2004) Mater Lett 58:757
4. Rajamathi M, Seshadri R (2002) Curr Opin Solid State Mater Sci 6:337
5. Lopez-Quintela MA (2003) Curr Opin Colloid Interface Sci 8:137
6. Bagwe RP, Khilar KC (1997) Langmuir 13:6432
7. Chen DH, Wu SH (2000) Chem Mater 12:1354
8. Curri ML, Agostiano A, Manna L, Della Monica M, Catalano M, Chiavarone L, Spagnolo V, Lugarà M (2000) J Phys Chem B 104:8391
9. Kuang D, Xu A, Fang Y, Ou H, Liu H (2002) J Cryst Growth 244:379
10. Husein M, Rodil E, Vera J (2003) Langmuir 19:8467
11. Mori Y, Okastu Y, Tsujimoto Y (2001) J Nanopart Res 3:219
12. Nanni A, Dei L (2003) Langmuir 19:933
13. Tai CY, Hsiao BY, Chiu HY (2004) Colloids Surf A: Physicochem Eng Aspects 237:105
14. Althues H, Kaskel S (2002) Langmuir 18:7428
15. Alberti G, Casciola M, Costantino U, Vivani R (1996) Adv Mat 8:291
16. Bellezza F, Cipiciani A, Costantino U, Negozio ME (2002) Langmuir 18:8737
17. Bellezza F, Cipiciani A, Costantino U (2003) J Mol Cat B:Enzym 26:47
18. Bellezza F, Cipiciani A, Costantino U, Nicolis S (2004) Langmuir 20:5019
19. Alberti G, Costantino U, Allulli S, Tomassini N (1978) J Inorg Nucl Chem 40:1113
20. Tai CY, Lee MH, Wu YC (2001) Chem Eng Sci 56:2389
21. Koppel DE (1972) J Chem Phys 57:4814
22. Berne BJ, Pecora R (1976) "Dynamic Light Scattering with Applications to Chemistry, Biology and Physics". Wiley, New York
23. Oszwaldowski S, Lipka R, Jarosz M (1998) Analytica Chimica Acta 361:177
24. Arriagada FJ, Osseo-Asare K (1995) J Colloid Interface Sci 170:8
25. Harelind Ingelsten H, Beziat JC, Bergkvist K, Palmqvist AEC, Skoiglundh M, Qiuhong H, Falk LKL, Holmberg K (2002) Langmuir 18:1811
26. Troup JM, Clearfield A (1977) Inorg Chem 16:3311
27. Lopez Perez JA, Lopez Quintela MA, Mira J, Rivas J, Charles SW (1997) J Phys Chem B 101:8045
28. Costantino U, La Ginestra A (1982) Termochim Acta 58:179